PCCP

Accepted Manuscript

This is an *Accepted Manuscript*, which has been through the Royal Society of Chemistry peer review process and has been accepted for publication.

Accepted Manuscripts are published online shortly after acceptance, before technical editing, formatting and proof reading. Using this free service, authors can make their results available to the community, in citable form, before we publish the edited article. We will replace this *Accepted Manuscript* with the edited and formatted *Advance Article* as soon as it is available.

You can find more information about *Accepted Manuscripts* in the Information for Authors.

Please note that technical editing may introduce minor changes to the text and/or graphics, which may alter content. The journal's standard Terms & Conditions and the Ethical guidelines still apply. In no event shall the Royal Society of Chemistry be held responsible for any errors or omissions in this *Accepted Manuscript* or any consequences arising from the use of any information it contains.

ROYAL SOCIETY OF CHEMISTRY

www.rsc.org/pccp

CREATED USING THE RSC LaTeX PCCP ARTICLE TEMPLATE – SEE www.rsc.org/electronicfiles FOR DETAILS
ARTICLE TYPE
www. rsc.org/xxxxxx | XXXXXXXX

Design Considerations for Enhancing Absorption in Semiconductors on Metals through Surface Plasmon Polaritons†

Christopher D. Bohn,*[a] Amit Agrawal,[b] Youngmin Lee,[a] Charles J. Choi,[c] Matthew S. Davis,[b] Paul H. Haney,[a] Henri J. Lezec,[a] and Veronika A. Szalai,*[a]

Received Xth XXXXXXXXXX 20XX, Accepted Xth XXXXXXXXX 20XX
First published on the web Xth XXXXXXXXXX 200X
DOI: 10.1039/b000000x

Surface plasmon polaritons have attracted attention for energy applications such as photovoltaic and photoelectrochemical cells because of their ability to improve optical absorption in thin films. We show that surface plasmon polaritons enhance absorption most significantly in materials with small positive real permittivity and large positive imaginary permittivity, *e.g.* organics or CdTe. Additional losses, accounting for dissipation in the metal and the existence of a cutoff frequency above which polaritons are no longer bound, are incorporated into efficiency calculations. Owing to these losses, devices with optical absorption based solely on SPPs will necessarily always have a lower efficiency than that predicted by the Shockley-Queisser limit. Calculations are presented for specific materials, including crystalline and amorphous Si, GaAs, CdTe, a P3HT:PCBM blend, α-Fe_2O_3 and rutile TiO_2, as well as for general materials of arbitrary permittivity. Guidelines for selecting absorber materials and determining whether specific materials are good candidates for improving optical absorption with SPPs are presented.

Surface plasmon polaritons (SPPs) are collective oscillations of the electromagnetic field which propagate along an interface between a metal and a dielectric with complex relative permittivities, ε_m and ε_d, respectively. The ability to spatially confine the electromagnetic field to an interface holds promise for a range of applications from nanoscale optical communications and switching[1,2] to realizing negative index metamaterials[3] for cloaking[4,5] and microscopy[6]. SPPs are important for energy applications, including photovoltaic[7] or photoelectrochemical devices[8], because they can be used to enhance absorption through concentrating the electromagnetic field in the absorber, and thus boost device efficiency, particularly in thin films where the length scale for minority carrier diffusion is less than that for photon absorption. Recently, several papers have investigated the thermodynamic limit to nanophotonic enhancement of light absorption[9–11]. These studies found that when nanophotonic strategies are employed, absorption enhancement - defined as the total absorption divided by the single pass absorption - can exceed $4n^2$ for illumination at normal incidence, where n is the real part of the complex refractive index of the active layer. In ultrathin materials, single pass absorption is small, meaning that the denominator of the enhancement calculation is nearly zero and large values of enhancement can easily be obtained. A more appropriate figure of merit for energy applications is the total fraction of incoming light that can be captured in the dielectric using nanophotonic light trapping strategies, or equivalently the absolute attainable energetic efficiency. Here, we outline the fundamental physical requirements for absorption with SPPs by solving Maxwell's equations for the simplest case, the interface between two semi-infinite materials. Our objective is to provide guidelines for selecting absorber materials and to determine which optical properties make materials good candidates for plasmonics. We demonstrate that optimum performance requires maximizing the imaginary part of the relative permittivity, $Im\{\varepsilon_d\}$, while minimizing the real part of the relative permittivity, $Re\{\varepsilon_d\}$. Interestingly, these considerations highlight the efficacy of using SPPs with organic PV materials as well as CdTe, but demonstrate the limitations of traditional absorbers including crystalline and amorphous Si, GaAs and oxides such as TiO_2 and α-Fe_2O_3 for which the ratio of $Re\{\varepsilon_d\}/Im\{\varepsilon_d\}$ is not favorable.

The predominant experimental approach merging plasmonics and photovoltaics[7,12] has been to coat existing cells with metallic nanoparticles that support localized surface plasmon modes and scatter light into guided modes of the underly-

† Electronic Supplementary Information (ESI) available: Mathematics for calculating the fractional power absorbed and overall efficiency are provided. See DOI: 10.1039/b000000x/

[a] *Center for Nanoscale Science and Technology, National Institute of Standards and Technology, Gaithersburg, Maryland 20899, United States. Fax: 301-975-2303; Tel: 301-975-3792 (VAS) 301-975-4236 (CDB); E-mail: veronika.szalai@nist.gov, christopher.bohn@nist.gov*
[b] *Department of Electrical Engineering and Computer Science, Syracuse University, Syracuse, New York 13244, United States.*
[c] *Material Measurement Laboratory, National Institute of Standards and Technology, Gaithersburg, Maryland 20899, United States.*

Physical Chemistry Chemical Physics Accepted Manuscript

Physical Chemistry Chemical Physics Accepted Manuscript

ing dielectric.[13] This strategy was first pursued by Stuart and Hall[14], and has been applied to Si[15,16], GaAs[17] and organic photovoltaics [18] among others. Because scattering is not the focus of the present article and because localized surface plasmon resonance occurs over a narrow frequency range for a single nanoparticle, compared to the broadband nature of surface plasmon polaritons, localized surface plasmon resonance will not be discussed further. Other light trapping strategies such as multilayer waveguides, dielectric slabs, photonic crystals,[19] or other physical phenomena such as hot carrier transport[8,20] which do not rely on SPPs will also not be considered. Strategies based on propagating SPPs have been most successful in organic materials.[21] Using a P3HT:PCBM absorber, Morfa *et al.*[22] increased photovoltaic efficiency from 1.3 % in planar device to 2.2 % using a nanostructured thin film of Ag. Kang *et al.*[23] developed a heterojunction organic cell containing a copper phthalocyanine electron donor and a C60 acceptor, and achieved absolute efficiency increase from 0.96 % in a planar device to 1.32 % in Ag nanowire plasmonic grating. These efficiencies, however, are still below the current record for single-junction organic PV devices of 11.1 %[24]. Improving efficiencies through surface plasmon polaritons has not, to date, resulted in record setting devices, suggesting that a close inspection of the underlying physics and limitations of SPPs is in order.

As a starting point to the mathematics, consider illumination of an interface between two semi-infinite materials, *e.g.* a dielectric on top of a metal, as shown in the inset of Fig. 1. The incident light can be described as the sum of its constituent transverse magnetic (TM) and transverse electric (TE) components. For example, the non-zero electric and magnetic field components for the TM case are $\mathrm{E}_x, \mathrm{E}_z$ and H_y. Solution of Maxwell's equations gives bound SPP modes for TM polarization only.[25,26] Assume a bound SPP mode propagating along the interface in the positive x-direction as an idealized starting point. This assumption ignores (i) the finite thickness of both the metal and dielectric layers in real devices, (ii) the initial absorption owing to light propagating through the dielectric towards the interface and (iii) imperfect coupling of the incoming plane wave to SPPs at the interface. While coupling efficiencies of incoming light to SPPs of greater than 45 % for TM polarized light have been reported[27], perfect coupling is unrealistic. Together these assumptions will therefore lead to an upper limit on the fraction of light which can be usefully absorbed using SPPs. For linear, isotropic media without external charge and current densities, the analytical solution for the electric field characterizing the SPP is given by the real component of the complex field (see Appendix A):

$$\mathbf{E}_\mathrm{m} = \left[\mathrm{E}_0, 0, -\mathrm{E}_0(\varepsilon_\mathrm{d}/\varepsilon_\mathrm{m})^{1/2}\right] e^{i\left(k_x x + k_{z,\mathrm{m}} z\right)} \tag{1a}$$

$$\mathbf{E}_\mathrm{d} = \left[\mathrm{E}_0, 0, \mathrm{E}_0(\varepsilon_\mathrm{m}/\varepsilon_\mathrm{d})^{1/2}\right] e^{i\left(k_x x - k_{z,\mathrm{d}} z\right)}, \tag{1b}$$

where $\mathbf{E}_\mathrm{m}$ and $\mathbf{E}_\mathrm{d}$ are the complex electric fields in the metal and dielectric, respectively, E_0 relates to the amplitude, k_x is the wavevector parallel to the interface and $k_{z,\mathrm{m}}$ and $k_{z,\mathrm{d}}$ are the wavevectors perpendicular to the interface in the metal and dielectric, respectively.

Of primary interest is the power which can be usefully absorbed for energy generation.[28] For linear media, the time-averaged dissipated power in the dielectric absorber owing to the SPP is given by:[29]

$$P_\mathrm{abs,d} = \frac{1}{2}\int_0^\infty\int_0^\infty Re\{\sigma\mathbf{E}_\mathrm{d}\cdot\mathbf{E}_\mathrm{d}^*\}dxdz = \frac{1}{2}\int_0^\infty\int_0^\infty \omega\varepsilon_0 Im\{\varepsilon_\mathrm{d}\}|\mathbf{E}_\mathrm{d}|^2 dxdz, \tag{2a}$$

where the factor of $1/2$ arises from time averaging, superscripted $*$ denotes the complex conjugate, $\sigma(\omega) = \omega\varepsilon_0 Im\{\varepsilon_\mathrm{d}\}$ is the real-valued conductivity, and

$$|\mathbf{E}_\mathrm{d}|^2 = |\mathrm{E}_0|^2\left(1+\frac{|\varepsilon_\mathrm{m}|}{|\varepsilon_\mathrm{d}|}\right)e^{2\left[-Im\{k_x\}x + Im\{k_{z,\mathrm{d}}\}z\right]}. \tag{3}$$

Note that for the definite integral in Eq. (2) to be bounded and nontrivial, $Im\{k_x\} > 0$ and $Im\{k_{z,\mathrm{d}}\} < 0$ are required. Overall, the power absorbed in the dielectric is calculated from Eqs. (2) and (3) to be:

$$P_\mathrm{abs,d} = -\frac{\omega\varepsilon_0 Im\{\varepsilon_\mathrm{d}\}|\mathrm{E}_0|^2}{8Im\{k_x\}Im\{k_{z,\mathrm{d}}\}}\left(1+\frac{|\varepsilon_\mathrm{m}|}{|\varepsilon_\mathrm{d}|}\right), \tag{4}$$

where $Im\{k_{z,\mathrm{d}}\} < 0$ ensures the expression is positive. A similar equation can be written for the metal. Taking the ratio of the dissipated power, $F_\mathrm{abs} = P_\mathrm{abs,d}/P_\mathrm{abs,m}$, gives:[28]

$$F_\mathrm{abs} = \frac{Im\{\varepsilon_\mathrm{d}\}}{Im\{\varepsilon_\mathrm{m}\}}\frac{|\varepsilon_\mathrm{m}|}{|\varepsilon_\mathrm{d}|}\frac{Im\{k_{z,\mathrm{m}}\}}{Im\{k_{z,\mathrm{d}}\}}. \tag{5}$$

The fractional power which is usefully captured by the absorber divided by the total power captured by both the metal and the dielectric absorber is $F_\mathrm{abs}/(F_\mathrm{abs}+1)$. For plasmonic applications involving light absorption, maximizing the ratio F_abs in Eq. (5) over the broadband solar spectrum is paramount. The relative power usefully absorbed can be considered the product of the field at the interface, the decay length of this field, and a material's ability to absorb. These quantities are represented in Eq. (5) by the terms $1/|\varepsilon_\mathrm{d}|$, $1/Im\{k_{z,\mathrm{d}}\}$ and $Im\{\varepsilon_\mathrm{d}\}$, respectively. Assuming $Re\{\varepsilon\} >> Im\{\varepsilon\}$, which holds for typical materials, Eq. 5 can be simplified using Eqs. (14) to

$$F_\mathrm{abs} \approx \frac{Im\{\varepsilon_\mathrm{d}\}}{Im\{\varepsilon_\mathrm{m}\}}\frac{Re\{\varepsilon_\mathrm{m}\}^2}{Re\{\varepsilon_\mathrm{d}\}^2}. \tag{6}$$

 This journal is © The Royal Society of Chemistry [year]

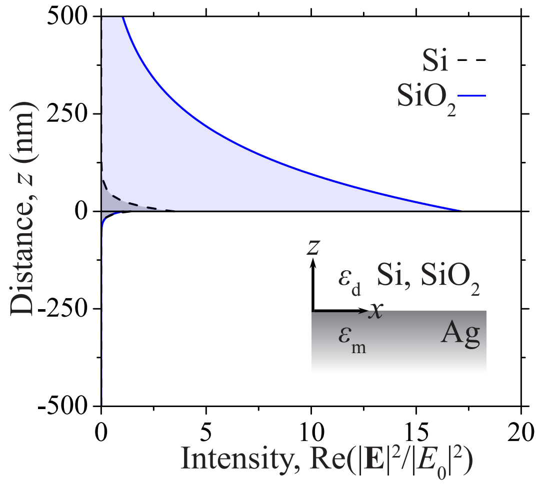

Fig. 1 Normalized intensity of the electromagnetic field as a function of distance from the interface between two semi-infinite media, shown schematically in the inset, for Ag and SiO_2 (blue, solid) and Ag and Si (black, dashed) at a free space wavelength of 830 nm. The SPP propagates in the positive x-direction; lines are drawn by evaluating Eq. (3) with $x = 0$.

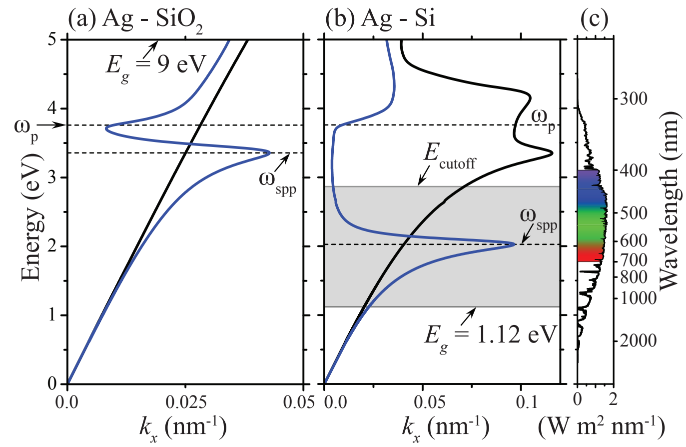

Fig. 2 Dispersion diagram showing photon energy *vs.* $Re\{k_x\}$ for (a) Ag and SiO_2 and (b) Ag and Si interfaces. The black curve corresponds to the light line in the dielectric $k_x = \sqrt{\varepsilon_d}\omega/c$; the blue curve shows $Re\{k_x\}$ calculated using Eq. (13). The larger $Re\{\varepsilon_d\}$ for Si relative to SiO_2 results in a significant reduction in the surface plasmon resonance frequency, ω_{spp}. To optimize absorption, the region between E_{cutoff} and E_g should maximally overlap with the solar spectrum plotted in (c).

On the metal side, Eq. (6) demonstrates that one should maximize $Re\{\varepsilon_m\}^2/Im\{\varepsilon_m\} = (n_m^2 - \kappa_m^2)^2/2n_m\kappa_m$ where $\varepsilon_m = (n_m + i\kappa_m)^2$. This is accomplished for $\kappa_m \to \infty$, which describes a perfect electrical conductor.

Practicably, the choice of a metal is limited to Al, Ag, Au, Cu and their alloys, *e.g.* AlCu.[30] These metals only behave as perfect electrical conductors with vanishing skin depths at terahertz frequencies and exhibit non-negligible skin depth at visible frequencies. Across the solar spectrum, Ag offers an optimal ratio of $Re\{\varepsilon_m\}^2/Im\{\varepsilon_m\}$ in Eq. (6) and, forgoing limitations of chemical stability, will be used as an illustrative metal in the remainder of this paper. For the dielectric absorber, one should maximize $Im\{\varepsilon_d\}/Re\{\varepsilon_d\}^2 = 2n_d\kappa_d/(n_d^2 - \kappa_d^2)^2$, which leads to $n_d = \kappa_d$. For the remainder of this paper, Eq. (5) will be used.

From Eq. (2), absorption is proportional to the intensity of the electromagnetic field, $|\mathbf{E}_d|^2$. Maximizing the integral of the field squared in the dielectric absorber is therefore the primary photonic objective. Under the assumption of a semi-infinite materials and noting that the intensity is a monotonically decreasingly exponential function in both materials, this objective is equivalent to maximizing both the intensity in the dielectric at the interface and the decay length of this intensity in the dielectric absorber. Fig. 1 shows the spatial profile of the time-averaged intensity normalized by the incident intensity for an interface between Ag and SiO_2 and for an interface between Ag and Si illuminated at a free space wavelength of 830 nm. Considering the Ag halfspace, it is evident that the electromagnetic intensity and its decay are nearly identical for both cases, as shown by overlapping curves in the bottom half of Fig. 1. In the dielectric halfspace, $Re\{\varepsilon_d\}$ is larger for Si than SiO_2 and both the interface value and the decay length of the electromagnetic field intensity is larger in SiO_2. The intensity at the interface is discontinuous and is given by $|\mathbf{E}_d(z=0^+)|^2/|\mathbf{E}_m(z=0^-)|^2 = |\varepsilon_m|/|\varepsilon_d|$, which is approximately $|Re\{\varepsilon_m\}|/|Re\{\varepsilon_d\}|$ when $|Re\{\varepsilon\}| >> |Im\{\varepsilon\}|$. Thus, for a fixed choice of metal, concentrating the intensity in the absorber at the interface requires minimizing its positive real permittivity. Next, to maximize the spatial extent of the field in the dielectric, we note that the ratio of decay lengths is given by $z_d/z_m = Im\{k_{z,m}\}/Im\{k_{z,d}\} = |Re\{\varepsilon_m\}|/|Re\{\varepsilon_d\}|$ from Eq. (14) for $|Re\{\varepsilon\}| >> |Im\{\varepsilon\}|$. On the absorber side, maximizing the integral of the exponentially decreasing intensity as in Eq. (2) requires maximizing its value at the interface as well as extending its decay length into the absorber, *viz.* minimizing the absorber's real positive permittivity.

For energy applications, it is necessary to maximize the frequency range over which SPPs can be supported and to ensure optimal overlap between this range and the solar spectrum. Figure 2 plots the dispersion diagram showing the relationship between $Re\{k_x\}$ and ω for the interface between Ag and either (a) SiO_2 or (b) Si, along with (c) the solar irradiance. The dispersion diagrams each display a light line corresponding to $k_x = \sqrt{\varepsilon_d}\omega/c$. Additionally, material specific parameters such as the energy corresponding to the bulk plasma frequency of the metal, ω_p, as well as the bandgap energy of

Physical Chemistry Chemical Physics Accepted Manuscript

the absorber, E_g, are labeled. From the dispersion diagrams, $Re\{k_x\}$ increases monotonically with ω up to a point termed the surface plasmon resonance frequency, ω_{spp}. Beyond this point, bound surface plasmons can mathematically exist until ω_{cutoff}, the frequency where one of the three necessary inequalities $Im\{k_{z,d}\} < 0$, $Im\{k_{z,m}\} < 0$ or $Im\{k_x\} > 0$ no longer holds. * Thus, the parameters ω_{spp} and ω_{cutoff} depend on both materials comprising the interface. The appropriate energy range over which SPPs exist and can contribute to absorption is limited by the lower bound of E_g and the upper bound of E_{cutoff}. SPPs with energy below E_g are not absorbed; while above E_{cutoff} SPPs do not exist as mathematically bound solutions. For optimal absorption, E_g should lie below the energy of the least energetic photon and E_{cutoff} should lie above the energy of the most energetic photon. For optimal efficiency, however, E_g of the single bandgap device should lie closer to the energy of maximum solar irradiance, 1.1 eV-1.3 eV, and E_{cutoff} should be maximized. We note that for the materials examined in this article, the cutoff energy typically coincides with the point where $Im\{k_{z,d}\} > 0$. Additionally, we note that in Fig. 2(a), the bandgap of SiO_2 of 9 eV lies outside the relevant frequency range for the solar spectrum and no cutoff frequency exists.

The previous sections demonstrated that minimizing the real permittivity of the dielectric increases the intensity of light in the absorber. Ultimately, however, the most important metric is the power that can be usefully absorbed in the dielectric. The ratio in Eq. (5) gives the power captured by the absorber divided by the power dissipated in the metallic support and, therefore, represents the objective function which must be maximized at each frequency to optimize absorption based on SPPs. Consider five independent variables: the frequency of incoming photons, the real and imaginary permittivity for the metal, and the real and imaginary permittivity for the dielectric absorber. Fixing the photon frequency and ε_m, a contour plot of absorption as a function of the real and imaginary parts of ε_d is shown in Fig. 3. Various real materials are labeled by specific points in the plot. For Ag at a free space wavelength of 500 nm, corresponding to the peak solar irradiance from the sun, it is evident that maximizing absorption requires maximizing the imaginary part of the permittivity of the absorber. The black line designates the contour where $F_{abs} = 2$ specifying the threshold above which 67 % of the incoming power is captured by the absorber. In Fig.3(a), the optical parameters for a-Si lie to the upper right of the plotted range. From Fig. 3(a), favorable absorption can be obtained with both organic absorbers such as P3HT:PCBM and II-VI semiconductors like CdTe. Rutile TiO_2, on the other hand, does not absorb

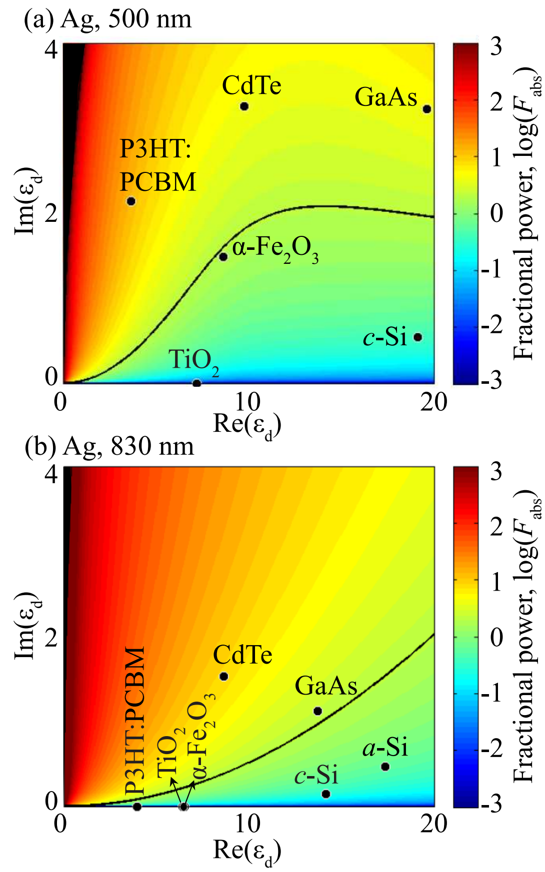

Fig. 3 Ratio of the power captured by the dielectric absorber divided by the power dissipated in the Ag support upon illumination by free space wavelengths of (a) 500 nm (2.5 eV) and (b) 830 nm (1.5 eV). The black line denotes the threshold where $F_{abs} = 2$ corresponding to power losses of 33 % in the metal. The leftmost black stripe represents points where $Im\{k_{z,d}\} > 0$.

* These inequalities arise from the restriction that the integral in Eq. (2) or its metallic counterpart must remain bounded. In general, several choices for the cutoff frequency exist including the surface plasmon frequency, ω_{spp}, the intersection of $Re\{k_x\}$ and the light line, or the bulk plasma frequency, ω_p.

This journal is © The Royal Society of Chemistry [year]
Physical Chemistry Chemical Physics Accepted Manuscript

at 500 nm because this energy of 2.5 eV is below the limiting badgap cutoff of $E_g = 3.1$ eV.[31] We note that Si does not have optimal real and imaginary permittivity for optical absorbtion enhancement using SPPs. The leftmost black stripe in the two plots shows regions where $Im\{k_{z,d}\} < 0$ is violated. At the longer wavelength of 830 nm, Fig. 3(b) again emphasizes the importance of maximizing $Im\{\varepsilon_d\}$ and minimizing $Re\{\varepsilon_d\}$ for increasing the power absorbed in the dielectric.

We next comment on the upper limits of power conversion efficiency from SPP enhanced absorption following the detailed balance method originally derived by Shockley and Queisser.[32] The efficiency, η_{SQ}, is calculated by maximizing the power generated by incoming photons while taking radiative recombination into account, as shown by Eqs. (22)-(24) in Appendix B. Calculation of a modified efficiency,$\eta_{SQ,spp}$, for the case of absorption through SPPs proceeds similarly. As always, there are losses associated with sub-bandgap excitations and the rapid thermalization of super-bandgap excitations. These result in a complete loss of the energy content of the solar spectrum below E_g, while harvesting only one E_g worth of energy at all other frequencies. Additionally, there is some degree of absorption and subsequent loss in the metal layer, and surface plasmon polaritons are only supported over a finite range of energies, setting an upper bound on the absorbed energy. Including these losses reduces the maximum efficiency from the Shockley-Queisser limit. Table 1 gives values of the Shockley-Quiesser efficiency, η_{SQ}, as well as the efficiency for purely plasmonic absorption with Ag as the chosen metal, $\eta_{SQ,spp}$. Details for the calculation of $\eta_{SQ,spp}$ are given in Appendix B. Efficiency is presented for a variety of semiconductor materials as well as for three hypothetical dielectric absorbers, D1, D2 and D3, whose complex permittivities are fixed with respect to frequency. Table 1 shows that absorbers such as CdTe and P3HT:PCBM, with small positive real permittivity and large positive imaginary permittivity, incur the least losses and display values of $\eta_{SQ,spp}$ which are closest to the theoretical Shockley-Quiesser limit. Comparing D3 to both D1 and D2 further supports this claim. The values for $\eta_{SQ,spp}$ represent the upper efficiency limits for devices where absorption occurs purely through SPPs. Using a different energy cutoff, *e.g.* corresponding to ω_{spp} rather than ω_{cutoff}, will lead to lower values of $\eta_{SQ,spp}$ since $\omega_{cutoff} > \omega_{spp}$. Only for the case of a perfect electrical conductor is the calculated plasmonic efficiency exactly equal to the Shockley-Quiesser limit, since the field is perfectly confined within the absorber. While the limiting efficiencies in Table 1 were derived for a 2D geometry where the incident light was linearly polarized (TM) to couple to SPPs, these presented efficiencies hold equally in 3D. For a 3D geometry, both TM and TE polarizations of incoming light can effectively couple to SPPs on the planar surface. The limiting efficiency derived for the 2D geometry with a single polarization will therefore be equivalent to that for the 3D geometry with a linear combination of two polarizations. Importantly then, the efficiency limits presented in Table 1 hold for both 2D and 3D geometries.

This article has demonstrated that minimizing positive real permittivity and maximizing positive imaginary permittivity of the dielectric are fundamental requirements for enhancing light absorption using surface plasmon polaritons. This guideline can be used to choose materials or to determine whether a particular material is a good candidate for plasmonic enhancement of optical absorption. Physically, these limitations suggests that plasmonic strategies hold promise for carbon-based nanomaterials including organic polymers, fullerenes, graphene and carbon nanotubes as well as for certain II-VI semiconductors like CdTe.[33] For several oxides (TiO_2, Fe_2O_3) used in photoelectrochemical applications and for traditional absorber materials (c-Si, a-Si, GaAs), SPP enhancement does not appear promising for enhancing absorption over the broad-band solar spectrum. While further improvements based on material combinations or patterning cannot be ruled out, these materials will likely be most useful in semiconductor sensing applications operating at a single, fixed frequency.[34] Experiments support these conclusions. Considering photoelectrochemical applications[35], research on α-Fe_2O_3 with Au plasmonic structures has resulted in either a decrease in absolute photocurrent[36] or low measured enhancement which persists at photon energies below the bandgap where the semiconductor cannot absorb[37,38]. These results support the theoretical difficulties identified in this article of improving absorption with SPPs in many real materials.

The previous analysis relied on several key assumptions: both the metal and the dielectric are semi-infinite, no power is absorbed as the incident light passes through the dielectric absorber on its way to the interface, and the incoming light perfectly couples to SPPs up to some cutoff energy, E_{cutoff}. Together these assumptions imply that $\eta_{SQ,spp}$ is a true upper bound limit on the efficiency for a device where absorption occurs through surface plasmon polaritons, defined mathematically as bound electromagnetic waves. Our assumptions place certain limitations on the conclusions. Specifically, if other absorption pathways, such as absorption prior to coupling to SPPs, are considered, higher efficiencies could be achieved. Extension to more complex multilayer geometries with finite thickness of absorber, metal and even cladding materials is also possible, but the conclusions presented here for a single, semi-infinite interface will still provide valuable guidelines.

In conclusion, surface plasmon polaritons can be used to enhance absorption in materials with small positive real permittivity and large positive imaginary permittivity. The first requirement stems from considerations of maximizing the relative integrated intensity in the absorber, which for a semi-infinite interface requires maximizing the field intensity at the interface and the decay length of this field in the absorber.

Physical Chemistry Chemical Physics Accepted Manuscript

Table 1 Table of the bandgap energy (E_g), cutoff energy for SPPs (E_{cutoff}), SPP energy corresponding to the local maximimum in $Re\{k_x\}$ from the dispersion diagram ($E_{spp} = h\omega_{spp}/2\pi$), Shockley-Queisser efficiency (η_{SQ}) and the limiting efficiency calculated for cases where absorption proceeds entirely through SPPs ($\eta_{SQ,spp}$), for crystalline and amorphous Si, GaAs, CdTe, a P3HT:PCBM blend, α-Fe_2O_3 and rutile TiO_2 as well as three fictitious materials with fixed, frequency-independent permittivities. References for the optical parameters of specific materials are listed. The parameters for Ag were taken from[39].

Material	E_g (eV)	E_{cutoff} (eV)	E_{spp} (eV)	η_{SQ} (%)	$\eta_{SQ,spp}$ for Ag (%)	Ref / Info
c-Si	1.12	2.88	2.03	31	7	[40]
a-Si	1.12	2.38	1.83	31	12	[41]
GaAs	1.42	2.58	2.02	31	15	[40]
CdTe	1.45	2.89	2.26	30	22	[41]
P3HT:PCBM	1.85	3.61	3.15	26	20	[42, 43]
α-Fe_2O_3	2.10	3.01	2.43	22	11	[44]
TiO_2	3.10	3.53	2.68	8	1	[45]
D1	1.12	2.34	3.45	31	21	$Re\{\varepsilon_d\} = 10$, $Im\{\varepsilon_d\} = 1$
D2	1.12	2.16	2.98	31	25	$Re\{\varepsilon_d\} = 10$, $Im\{\varepsilon_d\} = 4$
D3	1.12	2.54	3.00	31	28	$Re\{\varepsilon_d\} = 2.5$, $Im\{\varepsilon_d\} = 4$

Small real permittivity also ensures a large frequency range over which SPPs can be supported and, in practical devices, will reduce reflections at the interface between the external medium such as air owing to the smaller index of refraction. The second requirement for large imaginary permittivity or large extinction coefficient is necessary for absorption. An extensive parameter space covering a broad range of permittivities for the absorber has been investigated with Ag as the choice of metal owing to low SPP losses. Several material systems including oxides (TiO_2, Fe_2O_3) and traditional semiconductors (c-Si, a-Si, GaAs) have real permittivities too large and imaginary permittivities too low to be usefully considered for enhancing absorption through SPPs. In contrast, select II-VI semiconductors including CdTe as well as organic materials such as polymers, fullerenes, graphene and carbon nanotubes hold promise. Our calculations support this assertion and show that an upper limit for the absolute photovoltaic efficiency of approximately 20 % can be achieved in CdTe or a P3HT:PCBM blend when absorption proceeds entirely through surface plasmon polaritons.

This journal is © The Royal Society of Chemistry [year]

Physical Chemistry Chemical Physics Accepted Manuscript

A Appendix A

For linear, isotropic media without external charge and current densities, Maxwell's equations can be written as[26],

$$\nabla \cdot \mathbf{E} = 0 \tag{7a}$$
$$\nabla \cdot \mathbf{H} = 0 \tag{7b}$$
$$\nabla \times \mathbf{E} = -\mu_0 \mu \frac{\partial \mathbf{H}}{\partial t} \tag{7c}$$
$$\nabla \times \mathbf{H} = \varepsilon_0 \varepsilon \frac{\partial \mathbf{E}}{\partial t}, \tag{7d}$$

where μ and ε are, respectively, the relative permeability and permittivity of a material, $\mathbf{H}$ is the magnetic field, $\mathbf{E}$ is the electric field, t denotes time and the subscript $_0$ signifies vacuum. The boundary conditions for continuity of the normal and tangential components are[25],

$$\mathbf{n} \cdot (\varepsilon_0 \varepsilon_\mathrm{d} \mathbf{E}_\mathrm{d} - \varepsilon_0 \varepsilon_\mathrm{m} \mathbf{E}_\mathrm{m}) = 0 \tag{8a}$$
$$\mathbf{n} \cdot (\mu_0 \mu_\mathrm{d} \mathbf{H}_\mathrm{d} - \mu_0 \mu_\mathrm{m} \mathbf{H}_\mathrm{m}) = 0 \tag{8b}$$
$$\mathbf{n} \times (\mathbf{E}_\mathrm{d} - \mathbf{E}_\mathrm{m}) = 0 \tag{8c}$$
$$\mathbf{n} \times (\mathbf{H}_\mathrm{d} - \mathbf{H}_\mathrm{m}) = 0, \tag{8d}$$

where the subscripted d and m refer to the dielectric and metal, respectively.

Assuming harmonic time dependence ($\partial/\partial t = -i\omega$), homogeneity in the $y-$direction ($\partial/\partial y = 0$) considering the geometry in the inset of Fig. 1 and propagation along x for SPPs ($\partial/\partial x = ik_x$), Eqs. (7c) and (7d) yield[26]:

$$-\frac{\partial E_y}{\partial z} = i\omega\mu_0\mu H_x \tag{9a}$$
$$\frac{\partial E_x}{\partial z} - ik_x E_z = i\omega\mu_0\mu H_y \tag{9b}$$
$$ik_x E_y = i\omega\mu_0\mu H_z \tag{9c}$$

$$\frac{\partial H_y}{\partial z} = i\omega\varepsilon_0\varepsilon E_x \tag{10a}$$
$$ik_x H_z - \frac{\partial H_x}{\partial z} = i\omega\varepsilon_0\varepsilon E_y \tag{10b}$$
$$-ik_x H_y = i\omega\varepsilon_0\varepsilon E_z. \tag{10c}$$

Considering TM polarization with non-zero E_x, E_z and H_y only and using $\mu = 1$ for non-magnetic materials, rearranging Eqs. (10a), (10c), and substituting these results into Eq. (9b) gives[25,26]:

$$E_x = -i\frac{1}{\omega\varepsilon_0\varepsilon}\frac{\partial H_y}{\partial z} \tag{11a}$$
$$E_z = -\frac{k_x}{\omega\varepsilon_0\varepsilon} H_y \tag{11b}$$
$$0 = \frac{\partial^2 H_y}{\partial z^2} + \left[\left(\frac{\omega}{c}\right)^2 \varepsilon - k_x^2\right] H_y, \tag{11c}$$

where Eq. (11c) is recognized as the wave equation and $1/c^2 = \varepsilon_0\mu_0$ was used. Next, postulate that the solution for the magnetic field for this set of equations takes the form $H_{y,j} = A_j \exp i(k_x x \pm k_{z,j} z - \omega t)$ where the plus and minus sign correspond to the metal and dielectric half-spaces $j = \{m, d\}$, respectively. Returning to the boundary conditions and considering the normal vector in the z-direction according to the geometry in the inset of Fig. 1, Eq. (8), for TM polarization, gives:

$$\varepsilon_\mathrm{m} E_{z,\mathrm{m}} = \varepsilon_\mathrm{d} E_{z,\mathrm{d}} \tag{12a}$$
$$E_{x,m} = E_{x,d} \tag{12b}$$
$$H_{y,m} = H_{y,d}. \tag{12c}$$

Thus, continuity of $H_{y,j}$ requires that $A_\mathrm{m} = A_\mathrm{d}$. Substitution into the wave equation (11c) yields, $k_{z,\mathrm{m}}^2 = (\omega/c)^2\varepsilon_\mathrm{m} - k_x^2$ and $k_{z,\mathrm{d}}^2 = (\omega/c)^2\varepsilon_\mathrm{d} - k_x^2$. From continuity of $E_{x,j}$ and using Eq. (11a) then, $k_{z,\mathrm{d}}/k_{z,\mathrm{m}} = -\varepsilon_\mathrm{d}/\varepsilon_\mathrm{m}$, so that the dispersion relation as an explicit function of ω is obtained:

$$k_x^2 = \left(\frac{\omega}{c}\right)^2 \frac{\varepsilon_\mathrm{m}\varepsilon_\mathrm{d}}{\varepsilon_\mathrm{m} + \varepsilon_\mathrm{d}}. \tag{13}$$

It follows that,

$$k_{z,\mathrm{m}}^2 = \left(\frac{\omega}{c}\right)^2 \frac{\varepsilon_\mathrm{m}^2}{\varepsilon_\mathrm{m} + \varepsilon_\mathrm{d}} \tag{14a}$$
$$k_{z,\mathrm{d}}^2 = \left(\frac{\omega}{c}\right)^2 \frac{\varepsilon_\mathrm{d}^2}{\varepsilon_\mathrm{m} + \varepsilon_\mathrm{d}}, \tag{14b}$$

where the positive or negative root is chosen to ensure $Im\{k_{z,j}\} < 0$. Here, it is important to note that because the dielectric is an absorber, ε_d has an imaginary component which cannot be ignored in calculations. Using Eqs. (11a) and (11b), the final analytical solution for the electric field characterizing the SPP as a function of time and space is given by the real component of the complex field[46],

$$\mathbf{E}_\mathrm{m} = [\mathrm{E}_0, 0, \mathrm{E}_0(-k_x/k_{z,\mathrm{m}})]\, e^{i\left(k_x x + k_{z,\mathrm{m}} z - \omega t\right)} \tag{15a}$$
$$\mathbf{E}_\mathrm{d} = [\mathrm{E}_0, 0, \mathrm{E}_0(k_x/k_{z,\mathrm{d}})]\, e^{i\left(k_x x - k_{z,\mathrm{d}} z - \omega t\right)}, \tag{15b}$$

with k_x and $k_{z,j}$ given explicitly by Eqs. (13) and (14), respectively. Substitution of $(k_x/k_{z,\mathrm{m}}) = (\varepsilon_\mathrm{d}/\varepsilon_\mathrm{m})^{1/2}$ and $(k_x/k_{z,\mathrm{d}}) = (\varepsilon_\mathrm{m}/\varepsilon_\mathrm{d})^{1/2}$ and omitting time-dependence gives Eq. (1) in the main text.

The previous calculations for the power absorbed in the dielectric, Eq. (4), can be verified by considering the Poynting vector and power flow. Using Eq. (15b), the magnetic field in the dielectric absorber is obtained from Eq. (11b) and is given by the real component of $\mathbf{H}_\mathrm{d} = [0, -\mathrm{E}_0\omega\varepsilon_0\varepsilon_\mathrm{d}/k_{z,\mathrm{d}}, 0] \exp i(k_x x - k_{z,d} z - \omega t)$. The time-

Physical Chemistry Chemical Physics Accepted Manuscript

averaged Poynting vector, $\langle \mathbf{S} \rangle = Re\{\mathbf{E}_{\rm d} \times \mathbf{H}_{\rm d}^*\}/2$, is then:

$$\langle \mathbf{S} \rangle = \begin{bmatrix} Re\{\varepsilon_{\rm d}\}Re\{k_x\} - Im\{\varepsilon_{\rm d}\}Im\{k_x\} \\ 0 \\ -Re\{\varepsilon_{\rm d}\}Re\{k_{z,\rm d}\} + Im\{\varepsilon_{\rm d}\}Im\{k_{z,\rm d}\} \end{bmatrix} \frac{|\mathrm{E}_0|^2 \omega\varepsilon_0}{2|k_{z,\rm d}|^2} e^{2\left(-Im\{k_x\}x + Im\{k_{z,\rm d}\}z\right)}. \tag{16a}$$

The total power flowing through the surface surrounding the control volume, defined previously as the first quadrant of the Cartesian plane, is then,

$$P_{\rm flow,d} = -\underbrace{\int_0^\infty \langle \mathbf{S} \rangle \cdot (-\hat{x})\, dz}_{\rm x=0} - \underbrace{\int_0^\infty \langle \mathbf{S} \rangle \cdot (-\hat{z})\, dx}_{\rm z=0} - 0 - 0, \tag{17}$$

where $\hat{x}$ and $\hat{z}$ are unit normal vectors. Note that zero power flows into the control volume at the limits where $x = \infty$ or $z = \infty$, as indicated by the final two zeros in Eq. (17). Separating terms based on the real and imaginary components of the permittivity gives,

$$P_{\rm flow,d} = -\frac{|\mathrm{E}_0|^2 \omega\varepsilon_0}{8|k_{z,\rm d}|^2 Im\{k_x\}Im\{k_{z,\rm d}\}} \Big[2Re\{\varepsilon_{\rm d}\}\big(Re\{k_x\}Im\{k_x\} + Re\{k_{z,\rm d}\}Im\{k_{z,\rm d}\}\big) + 2Im\{\varepsilon_{\rm d}\}\big(Im\{k_x\}^2 + Im\{k_{z,\rm d}\}^2\big)\Big], \tag{18a}$$

Noting that $\varepsilon_{\rm d}(\omega/c)^2 = k_x^2 + k_{z,\rm d}^2$, it can be shown that,

$$Re\{\varepsilon_d\} = \left(\frac{c}{\omega}\right)^2 \big(Re\{k_x\}^2 + Re\{k_{z,\rm d}\}^2 - Im\{k_x\}^2 - Im\{k_{z,\rm d}\}^2\big), \tag{19a}$$

$$Im\{\varepsilon_d\} = 2\left(\frac{c}{\omega}\right)^2 \big(Re\{k_x\}Im\{k_x\} + Re\{k_{z,\rm d}\}Im\{k_{z,\rm d}\}\big). \tag{19b}$$

Dividing Eq. (19a) by Eq. (19b) and rearranging to give an explicit function of $Re\{\varepsilon_d\}$, which is then substituted into Eq. (18), gives,

$$P_{\rm flow,d} = -\frac{\omega\varepsilon_0 |\mathrm{E}_0|^2 \left(|k_x|^2 + |k_{z,\rm d}|^2\right) Im\{\varepsilon_{\rm d}\}}{8 Im\{k_x\}Im\{k_{z,\rm d}\}|k_{z,\rm d}|^2}, \tag{20}$$

Further simplifying using $|k_x|^2/|k_{z,\rm d}|^2 = |\varepsilon_{\rm m}|/|\varepsilon_{\rm d}|$, one obtains:

$$P_{\rm flow,d} = -\frac{\omega\varepsilon_0 Im\{\varepsilon_{\rm d}\}|\mathrm{E}_0|^2}{8Im\{k_x\}Im\{k_{z,\rm d}\}}\left(1 + \frac{|\varepsilon_{\rm m}|}{|\varepsilon_{\rm d}|}\right), \tag{21}$$

which confirms that the power absorbed in the dielectric calculated previously using Ohmic power dissipation over the volume, $P_{\rm abs,d}$ in Eq. (4), is equivalent to the energy balance considering power flow entering and leaving through the surface, Eq. (21).

B Appendix B

For photovoltaic energy conversion, the current density of the cell is given by:[32]

$$I(V) = q\frac{2\pi}{c^2h^3}\left[f\int_{E_{\rm g}}^{\infty} \frac{E^2 dE}{e^{\frac{E}{kT_{\rm s}}} - 1} - \int_{E_{\rm g}}^{\infty} \frac{E^2 dE}{e^{\frac{E-qV}{kT_{\rm c}}} - 1}\right], \tag{22}$$

where q is the elementary charge, c the speed of light in vacuo, h Planck's constant, k is Boltzmann's constant, V is the applied potential, $f = R_{\rm sun}^2/d_{\rm sun}^2$, where $R_{\rm sun}$ is the radius of the sun and $d_{\rm sun}$ is the distance between the earth and sun, $T_{\rm s} = 5780$ K is the temperature of the sun, and $T_{\rm c} = 300$ K is the ambient temperature of earth. In equation (22), the first term accounts for radiation the cell receives form the sun over a small solid angle. The second term accounts for the cell, biased at potential V, radiating as a blackbody at $T_{\rm c}$ over the hemisphere. Consistent with the original derivation[32], the blackbody radiation the cell receives at $T_{\rm c}$ from its surroundings is negligible relative to the incoming radiation from the sun and has been ignored. The total power density incident on the cell from the sun is given by the Stefan-Boltzmann equation:

$$P_{\rm sun} = \frac{2\pi^5 k^4}{15c^2h^3} T_{\rm s}^4 f. \tag{23}$$

Thus, the efficiency limit of Shockley and Queisser, defined as the power delivered to a matched load divided by the total incoming power, is given by:

$$\eta_{\rm SQ} = \max\left[I(V)V\right]/P_{\rm sun}. \tag{24}$$

For plasmonics, only a fraction of the incoming power or, equivalently, only a fraction of the incoming solar photons at each frequency is absorbed by the dielectric and not lost to the metal. Additionally, SPPs can only be supported from the bandgap energy $E_{\rm g}$ to some energy $E_{\rm cutoff}$, corresponding to a cutoff frequency $\omega_{\rm cutoff}$. When absorption proceeds strictly through SPPs, the current density is modified:

$$I_{\rm spp}(V) = q\frac{2\pi}{c^2h^3}\left[f\int_{E_{\rm g}}^{E_{\rm cutoff}} \left(\frac{F_{\rm abs}(E)}{F_{\rm abs}(E)+1}\right)\frac{E^2 dE}{e^{\frac{E}{kT_{\rm s}}} - 1} - \int_{E_{\rm g}}^{\infty} \frac{E^2 dE}{e^{\frac{E-qV}{kT_{\rm c}}} - 1}\right]. \tag{25}$$

Thus, the limiting efficiency when absorption proceeds entirely through SPPs is giveb by:

$$\eta_{\rm SQ,spp} = \max\left[I_{\rm spp}(V)V\right]/P_{\rm sun}. \tag{26}$$

For example, for $E_{\rm g} = 1.12$ eV corresponding to the bandgap of crystalline Si, $\eta_{\rm SQ} = 30.6$ %. To calculate the efficiency when absorption proceeds entirely through SPPs, further material specific information is required in addition to the bandgap energy. Calculation of $F_{\rm abs}$ and $E_{\rm cutoff}$ require the

This journal is © The Royal Society of Chemistry [year]
Physical Chemistry Chemical Physics Accepted Manuscript

permittivity of both the metal and absorber to be known. The revised efficiency, which accounts for absorption losses in the metal as well as the frequency cutoff constraint for SPPs, is then give by $\eta_{\mathrm{SQ,spp}} = \max\left[I_{\mathrm{spp}}(V)V\right]/P_{\mathrm{sun}}$. For example, for crystalline Si with $E_{\mathrm{g}} = 1.12$ eV and $E_{\mathrm{cutoff}} = 2.88$ eV, $\eta_{\mathrm{SQ,SPP}} = 6.9$ % as shown in Table 1.

C Acknowledgements

We acknowledge Nikolai Zhitenev, Fred Sharifi, Heayoung Yoon and Adam Kinney for invaluable discussions.

References

1 S. A. Maier, M. L. Brongersma, P. G. Kik, S. Meltzer, A. A. G. Requicha and H. A. Atwater, *Adv. Mat.*, 2001, **13**, 1501–1505.
2 J. A. Dionne, K. Diest, L. A. Sweatlock and H. A. Atwater, *NanoLett.*, 2009, **9**, 897–902.
3 T. Xu, A. Agrawal, M. Abashin, K. J. Chau and H. J. Lezec, *Nature*, 2013, **497**, 470–474.
4 D. Schurig, J. Mock, B. Justice, S. Cummer, J. Pendry, A. Starr and D. Smith, *Science*, 2006, **314**, 977–980.
5 A. Alù and N. Engheta, *Phys. Rev. Lett.*, 2008, **100**, 113901.
6 N. Fang, H. Lee, C. Sun and X. Zhang, *Science*, 2005, **308**, 534–537.
7 H. A. Atwater and A. Polman, *Nat. Mat.*, 2010, **9**, 205–213.
8 S. C. Warren and E. Thimsen, *Energy & Env. Sci.*, 2012, **5**, 5133–5146.
9 E. A. Schiff, *J. Appl. Phys.*, 2011, **110**, 104501.
10 J. N. Munday, D. M. Callahan and H. A. Atwater, *App. Phys. Lett.*, 2012, **100**, 121121.
11 Z. Yu, A. Raman and S. Fan, *PNAS*, 2010, **107**, 17491–17496.
12 V. E. Ferry, J. N. Munday and H. A. Atwater, *Adv. Mat.*, 2010, **22**, 4794–4808.
13 P. Spinelli and A. Polman, *Opt. Express*, 2012, **20**, 169431.
14 H. R. Stuart and D. G. Hall, *App. Phys. Lett.*, 1996, **69**, 2327–2329.
15 S. Pillai, K. Catchpole, T. Trupke and M. Green, *App. Phys. Lett.*, 2007, **101**, 093105.
16 D. Derkacs, S. Lim, P. Matheu, W. Mar and E. Yu, *App. Phys. Lett.*, 2006, **89**, 093103.
17 K. Nakayama, K. Tanabe and H. A. Atwater, *App. Phys. Lett.*, 2008, **93**, 121904.
18 J. Yang, J. You, C.-C. Chen, W.-C. Hsu, H. ren Tan, X. W. Zhang, Z. Hong and Y. Yang, *ACS Nano*, 2011, **5**, 6210–6217.
19 D. M. Callahan, J. N. Munday and H. A. Atwater, *Nano Lett.*, 2012, **12**, 214–218.
20 N. M. Gabor, J. C. W. Song, Q. Ma, N. L. Nair, T. Taychatanapat, K. Watanabe, T. Taniguchi, L. S. Levitov and P. Jarillo-Herrero, *Science*, 2011, **334**, 648–652.
21 A. E. Ostfeld and D. Pacifici, *Appl. Phys. Lett.*, 2011, **98**, 113112.
22 A. J. Morfa, K. L. Rowlen, T. H. R. III, M. J. Romero and J. van de Lagemaat, *App. Phys. Lett.*, 2008, **92**, 013504.
23 M.-G. Kang, T. Xu, H. J. Park, X. Luo and L. J. Guo, *Adv. Mat.*, 2010, **22**, 4378–4383.
24 L. L. Kazmerski, *NREL Best Research Cell Efficiencies*, `http://www.nrel.gov/ncpv/images/efficiency_chart.jpg`, 2013.
25 H. T. Baltar, K. Drozdowicz-Tomsia and E. M. Goldys, *Plasmonics - Principles and Applications*, InTech, 2012.
26 S. A. Maier, *Plasmonics: Fundamentals and Applications*, Springer, 2007.
27 S. T. Koev, A. Agrawal, H. J. Lezec and V. A. Aksyuk, *Plasmonics*, 2012, **7**, 269–277.
28 N. N. Lal, H. Zhou, M. Hawkeye, J. K. Sinha, P. N. Bartlett, G. A. Amaratunga and J. J. Baumberg, *Phys. Rev. B*, 2012, **85**, 245318.
29 J. D. Jackson, *Classical Electrodynamics*, John Wiley and Sons, Inc., 1962, p. 189.
30 M. N. Polyanskiy, *Refractive index database*, `http://refractiveindex.info`, 2013.
31 A. L. Lindsebigler, G. Lu and J. T. Y. Jr., *Chem. Rev.*, 1995, **95**, 735–758.
32 W. Shockley and H. J. Queisser, *J. Appl. Phys.*, 1961, **32**, 510–519.
33 M. A. Green, *Prog. Phtovolt: Res. Appl.*, 2011, **19**, 473–477.
34 M. E. Stewart, C. R. Anderton, L. B. Thompson, J. Maria, S. K. Gray, J. A. Rogers and R. G. Nuzzo, *Chem. Rev.*, 2008, **108**, 494–521.
35 S. Linic, P. Christopher and D. B. Ingram, *Nat. Mat.*, 2011, **10**, 911–921.
36 E. Thimsen, F. L. Formal, M. Grätzel and S. C. Warren, *NanoLett.*, 2012, **11**, 35–43.
37 H. Gao, C. Liu, H. E. Jeong and P. Yang, *ACS Nano*, 2012, **6**, 234–240.
38 I. Thomann, L. A. Pinaud, Z. Chen, B. M. Clemens, T. F. Jaramillo and M. L. Brongersma, *NanoLett.*, 2011, **11**, 3440–3446.
39 H.-J. Hagemann, W. Gudat and C. Kunz, *J. Opt. Soc. Am.*, 1975, **65**, 742–744.
40 E. D. Palik, *Handbook of Optical Constants of Solids I-III*, Academic Press, 1998.
41 *SOPRA n&k optical database*, `http://www.sspectra.com/sopra.html`, 2013.
42 F. Monestier, J.-J. Simon, P. Torchio, L. Escoubas, F. Flory, S. Bailly, R. de Bettignies, S. Guillerez and C. Defranoux, *Sol. Energy Mater. Sol. Cells*, 2007, **91**, 405–410.
43 J. R. Tumbleston, D.-H. Ko, R. Lopez and E. T. Samulski, *Proc. SPIE*, 2008, **7047**, 70470S.
44 H. Dotan, O. Kfir, E. Sharlin, O. Blank, M. Gross, Irina, Dumchin, G. Ankonina and A. Rothschild, *Nat. Mat.*, 2013, **12**, 158–164.
45 J. R. DeVore, *J. Opt. Soc. Am.*, 1951, **41**, 416–419.
46 J. A. Dionne, *PhD thesis*, California Institute of Technology, 2009.

This journal is © The Royal Society of Chemistry [year]

Physical Chemistry Chemical Physics Accepted Manuscript